

# Stellar Evolution with Rotation and Magnetic Fields

## IV: The Solar Rotation Profile

P. Eggenberger, A. Maeder, and G. Meynet

Observatoire de Genève, 51 chemin de Maillettes, CH-1290 Sauverny, Switzerland

Received ; accepted

**Abstract.** We examine the generation of a magnetic field in a solar-like star and its effects on the internal distribution of the angular velocity. We suggest that the evolution of a rotating star with magnetic fields leads to an equilibrium value of the differential rotation. This equilibrium is determined by the magnetic coupling, which favours a constant rotation profile, and meridional circulation which tends to build differential rotation. The global equilibrium stage is close to solid body rotation between about 0.7 and  $0.2 R_{\odot}$ , in good agreement with helioseismic measurements.

**Key words.** stars: rotation – stars: magnetic fields – stars: evolution

### 1. Introduction

One of the most severe problems in stellar physics concerns the rotation profile of the radiative interior of the Sun. Helioseismological results indicate that the angular velocity  $\Omega(r)$  is constant as a function of the radius  $r$  between about 20 % and 70 % of the total solar radius  $R_{\odot}$  (Brown et al. 1989; Kosovichev et al. 1997; Couvidat et al. 2003), while meridional and rotational turbulent diffusion (e.g. Zahn 1992) produce an insufficient internal coupling to ensure solid body rotation (Pinsonneault et al. 1989; Chaboyer et al. 1995). This suggests that another effect intervenes. Mestel & Weiss (1987) proposed that a weak internal magnetic field could provide the required internal coupling. Charbonneau & MacGregor (1993) also showed that large-scale internal magnetic fields can yield a weak internal differential rotation at the solar age. Another proposition to explain the flat rotation profile of the Sun is the angular momentum transport by internal gravity waves (Zahn et al. 1997; Talon et al. 2002; Talon & Charbonnel 2005).

An efficient dynamo has been proposed to operate in stellar radiative layers in differential rotation (Spruit 2002). This dynamo is based on the Tayler instability, which is the first one to occur in a radiative zone (Tayler 1973; Pitts & Tayler 1986). Even a very weak horizontal magnetic field is subject to Tayler instability, which then creates a vertical field component, which is wound up by differential rotation. As a result, the field lines become

progressively closer and denser and thus a strong horizontal field is created at the energy expense of differential rotation.

Maeder & Meynet (2003) studied the effects of the Spruit dynamo on the evolution of massive stars. They showed that a magnetic field can be created during the main sequence evolution of a rotating star by the Spruit dynamo and examined the timescale for the field creation, its amplitude and the related diffusion coefficients. Maeder & Meynet (2004) also developed a generalisation of the dynamo equations in order to encompass all cases of  $\mu$ - and  $T$ -gradients, as well as all cases from the fully adiabatic to non-adiabatic solutions. The clear result of these studies is that magnetic field and its effects are quite important in massive stars. The magnetic coupling, resulting from the Tayler–Spruit dynamo, is found to be able to enforce solid body rotation in massive stars. The question is now whether this dynamo also operates efficiently in a slow rotator like the Sun, so as to be responsible for the observed constancy of  $\Omega(r)$ .

In Sect. 2, we collect in a short consistent way the basic equations of the dynamo. In Sect. 3, the numerical models are presented, while Sect. 4 gives the conclusion.

### 2. The dynamo equations

In this section we briefly summarize the consistent system of equations for the dynamo (see Spruit 2002 and Maeder & Meynet 2004 for more details).

The energy density  $u_B$  of a magnetic field of intensity  $B$  per volume unity is

$$u_B = \frac{B^2}{8\pi} = \frac{1}{2} \rho r^2 \omega_A^2 \quad \text{with} \quad \omega_A = \frac{B}{(4\pi\rho)^{\frac{1}{2}} r}, \quad (1)$$

where  $\omega_A$  is the Alfvén frequency in a spherical geometry. In stable radiative layers, there is in principle no particular motions. However, if due to magnetic field or rotation, some unstable displacements of vertical amplitude  $l/2$  occur around an average stable position, the restoring buoyancy force produces vertical oscillations around the equilibrium position with a frequency equal to the Brunt–Väisälä frequency  $N$  (see Eq. 14 of Maeder & Meynet 2004 for the definition of  $N$  in a medium with both thermal and magnetic diffusivity  $K$  and  $\eta$ ).

The restoring oscillations will have an average density of kinetic energy

$$u_N \simeq f_N \rho l^2 N^2, \quad (2)$$

where  $f_N$  is a geometrical factor of the order of unity. If the magnetic field produces some instability with a vertical component, one must have  $u_B > u_N$ . Otherwise, the restoring force of gravity which acts at the dynamical timescale would immediately counteract the magnetic instability. From this inequality, one obtains  $l^2 < \frac{1}{2f_N} r^2 \frac{\omega_A^2}{N^2}$ . If  $f_N = \frac{1}{2}$ , we have the condition for the vertical amplitude of the instability (Spruit 2002; Eq. 6),

$$l < r \frac{\omega_A}{N}, \quad (3)$$

where  $r$  is the radius. This means that there is a maximum size of the vertical length  $l$  of a magnetic instability. In order to not be quickly damped by magnetic diffusivity, the vertical length scale of the instability must satisfy

$$l^2 > \frac{\eta}{\sigma_B} = \frac{\eta \Omega}{\omega_A^2}, \quad (4)$$

where  $\Omega$  is the angular velocity and  $\sigma_B$  the characteristic growth-rate of the magnetic field. In a rotating star, this growth-rate is  $\sigma_B = (\omega_A^2/\Omega)$  due to the Coriolis force (Spruit 2002; see also Pitts & Tayler 1986). The combination of the limits given by Eqs. (3) and (4) gives for the case of marginal stability,

$$\left(\frac{\omega_A}{\Omega}\right)^4 = \frac{N^2}{\Omega^2} \frac{\eta}{r^2 \Omega}. \quad (5)$$

The equality of the amplification time of Tayler instability  $\tau_a = N/(\omega_A \Omega q)$  with the characteristic frequency  $\sigma_B$  of the magnetic field leads to the equation (Spruit 2002)

$$\frac{\omega_A}{\Omega} = q \frac{\Omega}{N} \quad \text{with} \quad q = -\frac{\partial \ln \Omega}{\partial \ln r}. \quad (6)$$

By eliminating the expression of  $N^2$  between Eqs. (5) and (6), we obtain an expression for the magnetic diffusivity,

$$\eta = \frac{r^2 \Omega}{q^2} \left(\frac{\omega_A}{\Omega}\right)^6. \quad (7)$$

Eqs. (5) and (6) form a coupled system relating the two unknown quantities  $\eta$  and  $\omega_A$ . Instead, one may also consider for example the system formed by Eqs. (6) and (7). Formally, if one accounts for the complete expressions of the thermal gradient  $\nabla$ , the system of equations would be of degree 10 in the unknown quantity  $x = \left(\frac{\omega_A}{\Omega}\right)^2$  (Maeder & Meynet 2004). The fact that the ratio  $\eta/K$  is very small allows us to bring these coupled equations to a system of degree 4 (Maeder & Meynet 2004),

$$\frac{r^2 \Omega}{q^2 K} (N_T^2 + N_\mu^2) x^4 - \frac{r^2 \Omega^3}{K} x^3 + 2N_\mu^2 x - 2\Omega^2 q^2 = 0. \quad (8)$$

$K$  is the radiative diffusivity, namely  $K = \frac{4acT^3}{3\kappa\rho^2 C_p}$ . The solution of this equation, which is easily obtained numerically, provides the Alfvén frequency and by Eq. (7) the thermal diffusivity.

The azimuthal component of the magnetic field is much stronger than the radial one in the Tayler–Spruit dynamo. We have for these components (Spruit 2002)

$$B_\varphi = (4\pi\rho)^{\frac{1}{2}} r \omega_A \quad \text{and} \quad B_r = B_\varphi (l_r/r), \quad (9)$$

where  $\omega_A$  is the solution of the general equation (8) and  $l_r$  is given by Eq. (3).

Turning towards the transport of angular momentum by magnetic field, we first write the azimuthal stress by volume unity due to the magnetic field

$$S = \frac{1}{4\pi} B_r B_\varphi = \frac{1}{4\pi} \left(\frac{l_r}{r}\right) B_\varphi^2 = \rho r^2 \left(\frac{\omega_A^3}{N}\right). \quad (10)$$

Then, the viscosity  $\nu$  for the vertical transport of angular momentum can be expressed in terms of  $S$  (Spruit 2002),

$$\nu = \frac{S}{\rho q \Omega} = \frac{\Omega r^2}{q} \left(\frac{\omega_A}{\Omega}\right)^3 \left(\frac{\Omega}{N}\right). \quad (11)$$

This is the general expression of  $\nu$  with  $\omega_A$  given by the solution of Eq. (8). We have the full set of expressions necessary to obtain the Alfvén frequency  $\omega_A$  and the magnetic diffusivity  $\eta$ . Let us recall that  $\eta$  also expresses the vertical transport of the chemical elements, while the viscosity  $\nu$  determines the vertical transport of angular momentum by the magnetic field.

### 3. Stellar models

We consider here models of  $1 M_\odot$ , with the solar chemical composition of Grevesse & Sauval (1998). The stellar evolution code used for these computations is the Geneva code including shellular rotation (Meynet & Maeder 2005). We use the braking law of Kawaler (1988) in order to reproduce the magnetic braking undergone by low mass stars when arriving on the main sequence. Two parameters enter this braking law: the saturation velocity  $\Omega_{\text{sat}}$  and the braking constant  $K$ . Following Bouvier et al. (1997),  $\Omega_{\text{sat}}$  is fixed to  $14 \Omega_\odot$  and the braking constant  $K$  is calibrated

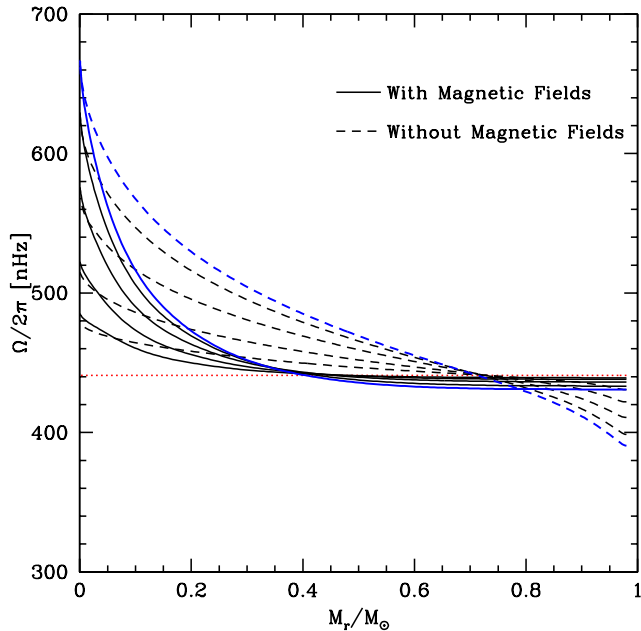


**Fig. 1.** Rotation profiles as a function of the lagrangian mass in solar units for models with (continuous lines) and without magnetic field (dashed lines). The dotted line indicates the initial solid body rotation on the ZAMS. The other lines correspond to an age of respectively 1, 2, 3, 4 and 4.57 Gyr.  $\Omega$  increases at the centre during the evolution on the main-sequence. No magnetic braking at the surface is included.

on the Sun. It is beyond the scope of the present paper to compute complete solar models reproducing the detailed solar structure deduced from helioseismic measurements. In this study, we simply focus on the evolution of the rotation profile of  $1 M_{\odot}$  models which reproduce the solar luminosity and radius at the age of the Sun (4.57 Gyr).

To investigate the effects of magnetic fields on the rotation profile of a slow rotating solar-like star, we first consider models without magnetic braking at the surface. Two models are computed: one with rotation only and a second with both rotation and magnetic field. The initial velocity of these models is approximately equal to the solar surface rotational velocity. Fig. 1 shows the evolution of the internal rotation profile for both models, starting from solid body rotation on the ZAMS. The rotation profile of the model with rotation only changes with time during the main sequence evolution due to the transport of angular momentum by circulation. As a result, the model with only rotation shows after 4.57 Gyr an angular velocity  $\Omega$  which is monotonically increasing when the distance to the centre decreases. The situation is quite different when magnetic fields are accounted for. As shown in Fig. 1, the angular velocity  $\Omega$  is almost constant between the surface and about  $0.3 M_{\odot}$ . In the central parts, the angular velocity increases due to the decrease of the horizontal coupling insured by the magnetic field strength resulting from the  $\mu$ -gradient in the stellar core ( $\nu$  varies like  $\nabla_{\mu}^{-2}$ ).

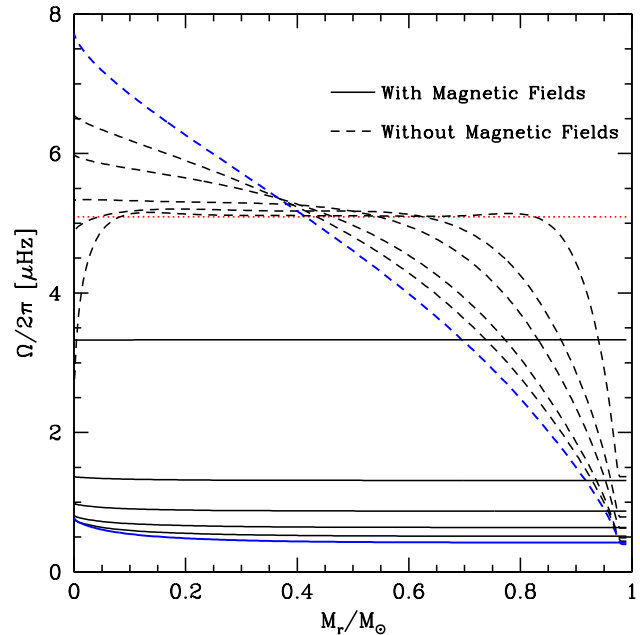


**Fig. 2.** Same as Fig. 1 but with an initial velocity of  $20 \text{ km s}^{-1}$ . The dotted line indicates the initial solid body rotation on the ZAMS. The other lines correspond to an age of respectively 0.1, 0.5, 1, 2, 3 and 4.57 Gyr. The surface angular velocity decreases when the star evolves due to the magnetic braking at the surface

As a second step, models with initial velocities of 20 and  $50 \text{ km s}^{-1}$  are computed. The braking law of Kawaler (1988) is used for these models in order to reproduce the solar surface rotational velocity. Fig. 2 compares the evolution of the internal rotation profile of models with only rotation and with both rotation and magnetic fields, starting with  $v_{\text{ini}} = 20 \text{ km s}^{-1}$  on the ZAMS. We notice that the surface rotation velocity rapidly decreases due to the magnetic braking at the surface. For the model including only rotational effects, this results in a large differential rotation reaching a factor of about 20 between the angular velocity at the surface and in the stellar core at the age of the Sun, in good agreement with the previous results of Chaboyer et al. (1995), but in contradiction with the flat rotation profile of the Sun. Fig. 2 shows that the model with both rotation and magnetic fields displays an almost constant angular velocity throughout the radiative interior, with only a small increase of  $\Omega$  in the central parts (for  $M_r \leq 0.2 M_{\odot}$ ). Fig. 3 better compares the theoretical rotation profiles of models computed with an initial velocity of  $50 \text{ km s}^{-1}$  to the one deduced from helioseismic measurements (Couvidat et al. 2003). Note that the rotation profiles of models with an initial velocity of  $50 \text{ km s}^{-1}$  are very similar to those with  $v_{\text{ini}} = 20 \text{ km s}^{-1}$ . The only difference is that models with  $v_{\text{ini}} = 50 \text{ km s}^{-1}$  exhibit slightly faster rotating cores than those computed with  $v_{\text{ini}} = 20 \text{ km s}^{-1}$ . Fig. 3 clearly shows that the rotation profile of models including both rotation and magnetic fields is in good agreement with the helioseismic measure-

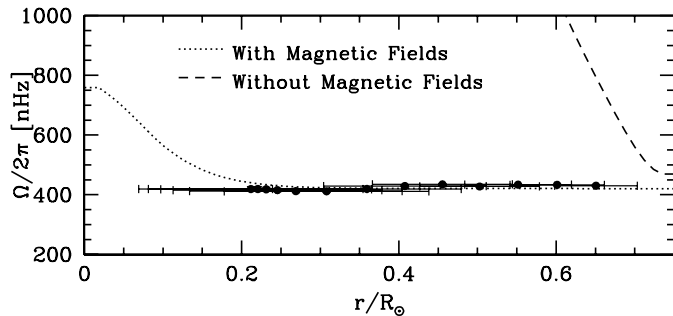


**Fig. 3.** Rotation profile for a model with rotation only (dashed line) and with both rotation and magnetic field (dotted line) at the age of the Sun. The initial velocity is  $50 \text{ km s}^{-1}$ . The points with their respective error bars correspond to the angular velocities in the solar radiative zone deduced from GOLF+MDI and LOWL data (Couvidat et al. 2003).

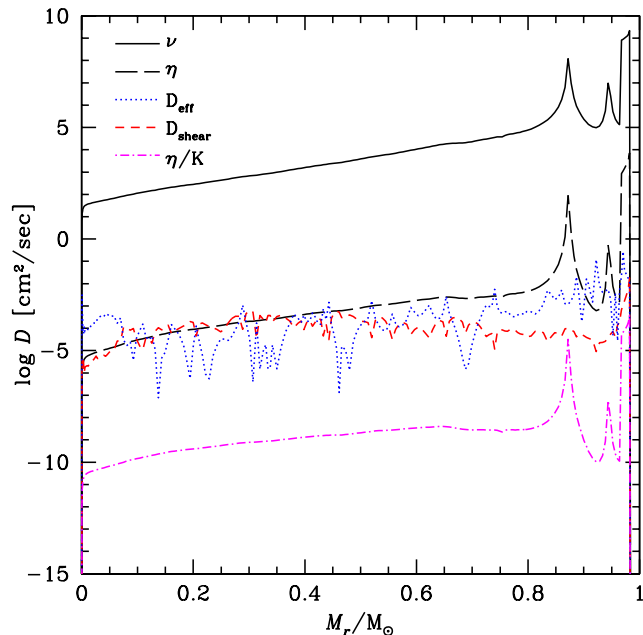


**Fig. 4.** Diffusion coefficients in the model with both rotation and magnetic fields and  $v_{\text{ini}} = 50 \text{ km s}^{-1}$  at the age of the Sun.

ments, while models with only rotation predict a too fast increase of  $\Omega$  when the distance to the centre decreases.

Finally, the values of the various diffusion coefficients for the model with magnetic fields and  $v_{\text{ini}} = 50 \text{ km s}^{-1}$  are shown in Fig. 4. The largest diffusion coefficient is  $\nu$  which acts for the vertical transport of angular momentum. The large value of  $\nu$  imposes the nearly constant  $\Omega$  in the interior and confirms the dominant role of the magnetic field for the transport of angular momentum. The numerical value for the azimuthal component of the field  $B_\varphi$  is of the order of a few  $10^2 \text{ G}$ . We also notice the small value of the coefficient of the shear turbulent mixing  $D_{\text{shear}}$ . Indeed, it is of the same order of magnitude as the

coefficient  $D_{\text{eff}}$ , which applies to the transport of chemical elements by meridional circulation, while in a rotating star without magnetic field  $D_{\text{shear}}$  is generally much larger (about 4 orders of magnitude). This small value is a consequence of the near solid body rotation of magnetic models and suggests that, for slow rotating solar-like stars, the rotation induced mixing is less efficient in magnetic models than in models with rotation only. This seems to be in agreement with observations. A detailed study of the evolution of trace elements like lithium and  $^3\text{He}$  with and without magnetic field will be needed to really investigate this point. Fig. 4 also shows that the value  $\eta/K$  is always very small, which justifies the simplifications made in deriving Eq. (8).

## 4. Conclusion

The main result of this study is that the Tayler–Spruit dynamo can account for the flat rotation profile of the Sun as deduced from helioseismic measurements. There remains however some doubts whether this dynamo is really active in stellar interiors, since 3D simulations have not yet confirmed the existence and efficiency of this particular instability; these simulations show a delicate balance between the generation of the instabilities and their relaxation to stable configurations (Braithwaite & Spruit 2004). It is also worthwhile to recall that magnetic field is not the only explanation, since purely hydrodynamical stellar models including the transport by internal gravity waves constitute another promising alternative.

*Acknowledgements.* We thank S. Couvidat and T. Corbard for providing us with the helioseismic rotation profile. We also thank S. Turck-Chièze, C. Charbonnel and S. Talon for useful discussions. Part of this work was supported financially by the Swiss National Science Foundation.

## References

- Bouvier, J., Forestini, M., & Allain, S. 1997, *A&A*, 326, 1023
- Braithwaite, J., & Spruit, H.C. 2004, *Nature*, 431, 819
- Brown, J.M., Christensen-Dalsgaard, J., Dziembowski, W.A., et al. 1989, *ApJ*, 343, 526
- Chaboyer, B., Demarque, P., & Pinsonneault, M.H. 1995, *ApJ*, 441, 865
- Charbonneau, P., & MacGregor, K.B. 1993, *ApJ*, 417, 762
- Couvidat, S., García, R.A., Turck-Chièze, S., et al. 2003, *ApJ*, 597, 77L
- Grevesse, N., & Sauval, A.J. 1998, *Space Sci. Rev.*, 85, 161
- Kawaler, S.D. 1988, *ApJ*, 333, 236
- Kosovichev, A., Schou, J., Scherrer, P.H., et al. 1997, *Sol. Phys.*, 170, 43
- Maeder, A., Meynet, G. 2003, *A&A*, 411, 543
- Maeder, A., Meynet, G. 2004, *A&A*, 422, 225
- Mestel, L., & Weiss, N.O. 1987, *MNRAS*, 226, 123
- Meynet, G., Maeder, A. 2005, *A&A*, 429, 581
- Pinsonneault, M.H., Kawaler, S.D., Sofia, S., & Demarque, P. 1989, *ApJ*, 338, 424
- Pitts, E., Tayler, R.J. 1986, *MNRAS*, 216, 139
- Spruit, H.C. 2002, *A&A*, 381, 923

- Talon, S., & Charbonnel, C. 2005, A&A in press, astro-ph:0505229
- Talon, S., Kumar, P., & Zahn, J.P. 2002, ApJ, 574, 175L
- Tayler, R.J. 1973, MNRAS, 161, 365
- Zahn, J.P. 1992, A&A, 265, 115
- Zahn, J.P., Talon, S., & Matias, J. 1997, A&A, 322, 320